Geophys. J. Int. (2006) **166,** 461–468 doi: 10.1111/j.1365-246X.2006.02940.x

Geothermal evidence for fluid flow through the gas hydrate stability field off Central Chile—transient flow related to large subduction zone earthquakes?

Ingo Grevemeyer,[1] Norbert Kaul[2] and Juan L. Diaz-Naveas[3]

[1]*IFM-GEOMAR, Leibniz Institut für Meereswissenschaften, Wischhofstraße* 1–3*,* 24148 *Kiel, Germany. E-mail: igrevemeyer@ifm-geomar.de*
[2]*Fachbereich Geowissenschaften, Universität Bremen, Klagenfurter Straße,* 28359 *Bremen, Germany*
[3]*Escuela de Ciencias del Mar, Universidad Católica de Valparaíso, Av. Altamirano* 1480*, Valparaíso, Chile*

Accepted 2006 January 30. Received 2005 November 18; in original form 2004 April 19

SUMMARY

Fluids are suspected to play a major role in the nucleation and rupture propagation of earthquakes. In Chile, seismological data were previously interpreted to indicate that fluids captured in the fault zone are released periodically during large underthrust earthquakes, leading to post-seismic fluid flow. In central Chile, heat flow derived from the presence of a bottom simulating reflector (BSR) show a smooth trend across the margin. BSR-derived data are in excellent agreement with thermal subduction zone models. Over the young accretionary prism, both BSR-derived and measured surface heat flow support a common trend. Landwards of the backstop, however, measured heat flow triples over a distance of 20–30 km, producing a profound discrepancy to the BSR-derived data. We suggest that this disparity is related to transient flow of warm fluids through the gas hydrate stability zone possibly caused by fluids released after large underthrust earthquakes. Such flow events may inherently affect the distribution of solid gas hydrates between the seafloor and the BSR.

Key words: earthquakes, fluids in rocks, gas hydrates, heat flow, subduction zone.

INTRODUCTION

Heat flow measurement on the surface of an active subduction zone and accretionary complex provide a critical boundary condition for the assessment of heat sources and related processes occurring within and below the major components of the margin wedge. For example, the updip and downdip limits of rupture during great subduction zone underthrust earthquakes are suggested to be controlled by the thermal state of the subduction thrust fault (e.g. Hyndman & Wang 1993; Oleskevich *et al.* 1999). Such deep seated processes are generally reflected in the regional long wavelength heat flow trend. Local variations in the heat flow are likely to reflect focused fluid flow along faults or other structurally controlled pathways (e.g. Foucher *et al.* 1990; Ganguly *et al.* 2000). The expulsion of pore fluids at accretionary complexes is related to the tectonic stacking of thrust slices of high-porosity and hence water-rich sediments, which dewater while the sediments are tectonically compressed and incorporated into the accretionary prism. Dewatering and hence advective heat transfer is generally most vigorous near the toe of accretionary complexes (e.g. Foucher *et al.* 1990; Fisher & Hounslow 1990). Further landwards, on the middle slope, measured heat flow is generally expected to be governed by conduction of heat, though locally, crustal scale faults cutting through the entire margin wedge may allow fluid backflow out of the deep subduction zone (Moore & Vrolijk 1992; Kopf *et al.* 2001), creating dewatering features like mud volcanoes or diapirs (e.g. Kopf 2002). The activity of such features is generally episodic and often related to great subduction zone earthquakes (Harrison 1944; Sondhi 1947).

In 2003 March we conducted a detailed geothermal study of the middle continental slope of Central Chile between the cities of Valparíso and Concepcíon aboard the Chilean Navy research vessel Vidal Gormaz (Fig. 1). The survey was dedicated to study the thermal state of gas hydrate bearing sediments, which have been seismically imaged in the region under ∼600 m to ∼2800-m-deep seafloor (Bangs & Cande 1997; Grevemeyer *et al.* 2003). Initial thermal constraints on the heat flow pattern of the region were derived from the temperature- and pressure-controlled depth of the gas hydrate stability field, as imaged by a bottom simulating reflector (BSR) (Grevemeyer *et al.* 2003). The overall BSR-derived heat flow trend supports a deep seated origin of the major heat source, which is controlled by the advection of heat into the subduction zone by the downgoing slab. The new measured data, however, show robust heat flow pattern along a 300 km stretch of the margin, with values which triple rapidly from 35–40 mW m^{-2} over the landward limit of the 1–2 Myr old accretionary prism to values of $>$100 mW m^{-2} over continental basement rocks. The short wavelength of the anomaly and its discrepancy to the BSR-derived data suggest a shallow origin, perhaps related to fluid flow. The following study examines possible sources of heat, which may explain the observations.

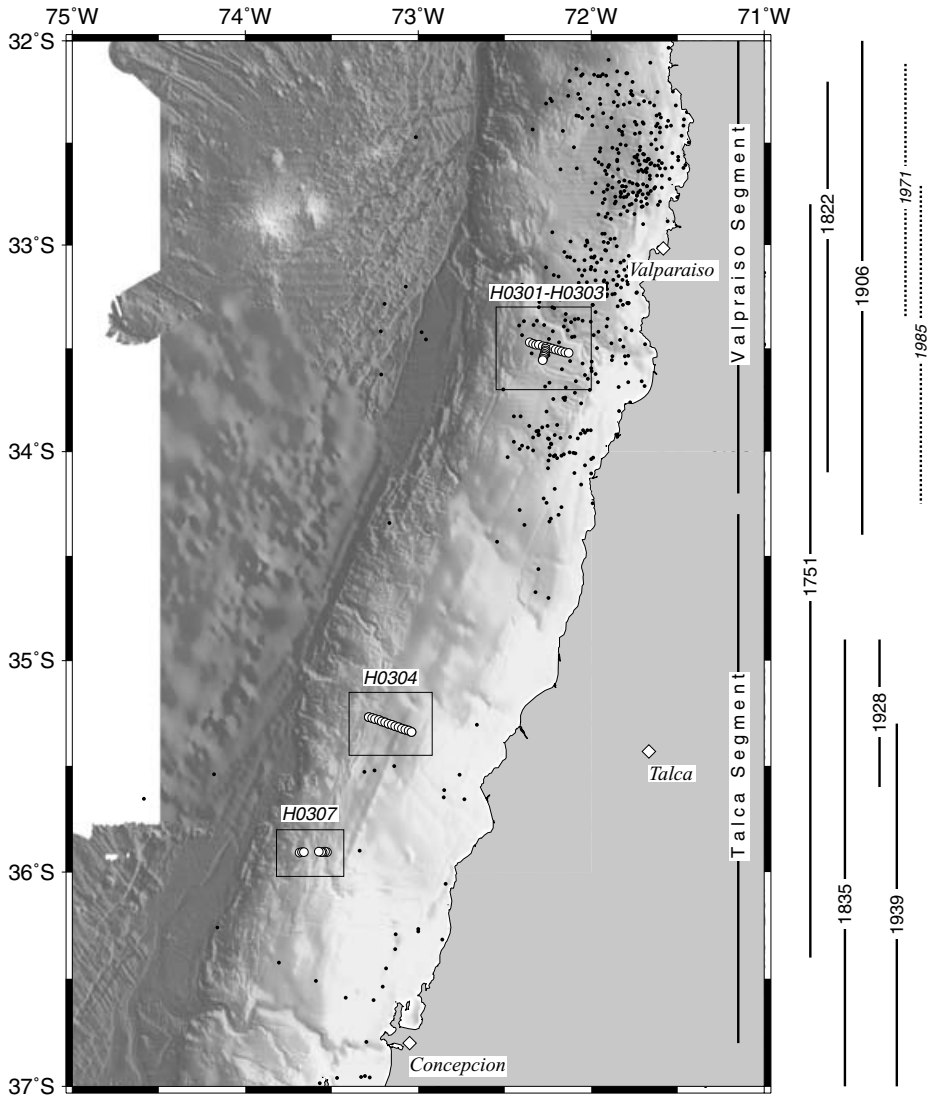

Figure 1. Topography and seismicity of the study area. Earthquakes (black dots) are from the catalogue of Engdahl & Villasenor (2002). Heat flow data (white circles) were obtained along three corridors between the cities of Valparaíso and Concepción. Labelled bars on the right-hand side of the figure show the year and width of the rupture area of great and large subduction zone earthquakes (Kelleher 1972; Christensen & Ruff 1986).

TECTONIC FRAMEWORK

In Central Chile, between 32°S and 37°S, the roughly 36 Myr old Nazca plate is subducted at a rate of ∼80 mm y^{-1} (DeMets *et al.* 1994). The area of Valparaíso is seismically one of the most active regions worldwide. Great earthquakes ($M > 8.0$) occur roughly every 90 yr, the last one in 1906. Moreover, a constant level of seismicity ($M > 4.0$) (Engdahl & Villasenor 2002) is characteristic for the area. The segment to the south of 34°S is seismically very quite, which is indicated by a lack of smaller earthquakes (Engdahl & Villasenor 2002). However, in the 20th century, two $M > 8.0$ earthquakes hit the region in 1928 and 1939. All great earthquakes of the 20th century ruptured different asperities (Fig. 1): the 1906 event the area north and south of Valparaíso, the 1928 earthquake the adjacent segment to the south, and the 1939 event the area immediately to the north of the Arauco peninsula (Kelleher 1972). Previous events occurred in 1528, 1751 and 1822. However, the low seismicity of the region south of 34°S suggests that the southern segment is now fully locked. The segment to the south of Concepción ruptured in 1960 during the largest earthquake ever recorded by seismic instruments (Ruff 1996). Like for the segment between Valparaíso and Concepción, the low level of seismicity indicates a locked subduction thrust.

The geology of the central Chile margin has been revealed by field mapping of on-shore exposures, aeromagnetic data, marine seismic reflection surveys and offshore exploration drilling. Exposed on-land are continental basement rocks, which have been interpreted as low-grade meta-sedimentary rocks that were part of a Palaeozoic accretionary wedge (Mordojovich 1974; Pankhurst *et al.* 1992). Basement rocks are intruded by Late Jurassic to Miocene plutons. Four forearc sedimentary basins have been identified between 35°S to 40°S (Mordojovich 1974). The oldest sediments drilled in the basins northwards of 38°S are Senonian while to the south the oldest sediments are only Miocene. Beneath metamorphic basement was found, the same that outcrops on-land. The young accretionary wedge, 20–30 km wide, abuts the truncated continental basement that extends seawards from beneath the shelf (von Huene 1997; Bangs & Cande 1997; Grevemeyer *et al.* 2003). According to this interpretation the age of the backstop is at least Eocene north of

~38°S, and Miocene to the south. The small size of the new accretionary prism, the subduction rate, and the style of deformation suggests that the current rapid rate of accretion can not have lasted more than 1–2 Myr (Bangs & Cande 1997).

THE GEOTHERMAL FIELD PROGRAMME

Vertical temperature gradients in the seafloor were measured using the 3-m-long University of Bremen 'violin-bow' design heat probe (e.g. Villinger *et al.* 2002). The gradient is obtained by inverting the decay of the frictional heating pulse (Hartmann & Villinger 2002), which is caused when the instrument penetrates the seafloor. At every other station, *in situ* conductivity measurements were made by applying a 20 s pulse of electric current along heater wires within the lance. The thermal decay of this calibrated heat pulse allows to estimate the conductivity at the location of *in situ* temperature measurements. Data from all 11 individual sensors were monitored in real time using a 2500-m-long coaxial cable connecting the probe with the ship. All individual temperature and conductivity measurements were inverted to obtain surface heat flow. The complete processing sequence to obtain surface heat flow is described elsewhere (Hartmann & Villinger 2002).

Heat flow data have been obtained along three transects near 33.5°S, 35.3°S and 35.8°S (Fig. 1). Each transect was located with respect to the interpretation of seismic data (Bangs & Cande 1997; Grevemeyer *et al.* 2003). The most detailed survey was conducted in the Valparaíso transect near 33.5°S. The first penetration was obtained on the easternmost tip of the young accretionary prism at 2400 m depth; the last penetration above continental basement near the shelf edge at 900 m depth. To detect the along slope variability, we obtained a cross line at roughly 1500 m depth. Two additional lines surveyed the area to the north of Concepción, covering 2000 to 600 m deep seafloor. Both stations were located above continental basement, but terminated near the landward limit of the young accretionary wedge. The spacing between individual penetrations was generally 1 nautical mile. Data are summarized in Table 1.

RESULTS

Along all transects similar pattern have been obtained (H0301, H0303, H0304, H0307). Heat flow is generally lowest on the most seaward stations (34–40 mW m^{-2}), and increases landwards (Figs 2 and 3), to triple within 15–25 km (110–140 mW m^{-2}). The robustness of this trend is supported by the along slope profile obtained perpendicular to the Valparaíso corridor (H0302). All nine penetrations provide almost constant values (51–57 mW m^{-2}) along a 10-km-long stretch. For almost all penetrations the thermal gradients were linear, indicating conductive transfer of heat through the margin wedge. Nevertheless, it is important to note that advection rates of less than ~1 cm yr^{-1} cannot be discriminated from pure conductive heat transfer by thermal measurements (Bredehoeft & Papadopulos 1965; Grevemeyer *et al.* 2004); thus, areas characterized by elevated heat flow may indicate locations of fluid outflow. However, the two most landward penetrations of the 35.3°S transect provide curved gradients, which may either indicate the impact of seasonal variations of the temperature in the bottom water layer, or may indicate vertical migration of fluids and hence advection of heat. Although we can not rule out the impact of temperature variation in the bottom water on the thermal gradient, the excellent fit of advective profiles to measurements from two different sites may support that advection is governing the curvature of the thermal gradients (Fig. 2). Both temperature profiles can be best explained by seepage of fluids at rates of 20–40 cm y^{-1} (Bredehoeft and Papadopulos 1965). Therefore, it seems reasonable to assume that shallow fluid flow is responsible to cause the prominent short wavelength heat flow anomaly.

A comparison of BSR-derived heat flow with the measured heat flow anomaly indicates an almost flat trend for the BSR-derived heat flow (Fig. 3a), which is in excellent agreement with a descending lithosphere with little generation of shear heating in the subduction thrust (Grevemeyer *et al.* 2003). Models with shear heating in the seismogenic zone (e.g. Molnar & England 1990) do produce heat flow trends that increase landwards. However, the rapid change and hence short wavelength trend of the measured data could not be reproduced by reasonable shear stresses in the fault zone. Furthermore, lateral changes of shear stress would affect both measured and BSR-derived heat flow. The most likely cause of the anomaly and its discrepancy to BSR-derived values is, therefore, shallow fluid flow between the BSR and the seafloor (e.g. Davis *et al.* 1990; Grevemeyer *et al.* 2004).

DISCUSSION AND CONCLUSIONS

The three corridors studied during the *Vidal Gormaz* survey provide similar features. However, the most homogeneous data set was obtained along the Valparaíso transect near 33.5°S. For discussion, we will, therefore, concentrate on that corridor. Off Valparaíso, BSR-derived and measured heat flow are in excellent agreement over the young accretionary complex (Fig. 3a). Over the continental basement (or an old accretionary prism), however, measured and BSR-derived data indicate different trends. The BSR-derived heat flow remains almost constant across the slope (in agreement with subduction zone models), while the measured heat flow increases profoundly landwards. Heat flow values that increase landwards could be forced by high shear stress in the subduction thrust or by an increase of radioactive heat production in the continental backstop. Both processes, however, are deep seated and would, therefore, also affect the BSR-derived data. To explain similar heat flow pattern elsewhere, it was suggested that the discrepancy might be related to fluid flow between the BSR and the seafloor (e.g. Davis *et al.* 1990; Grevemeyer *et al.* 2004). Fluid flow through the gas hydrate stability field may occur where warm fluids move relatively quickly through permeable settings and keep the surrounding sediments warm enough to prevent gas hydrate formation. Such settings have been imaged seismically elsewhere (Wood *et al.* 2002). Nevertheless, if the fluid flow system would be steady state, BSR-derived and measured values should support a common trend. We, therefore, hypothesize that the observed features support a transient fluid flow regime, perhaps linked to the cycle of large subduction zone thrust earthquakes.

First, however, we like to discuss an alternative fluid flow regime. At continental margins the topographic gradient between coastal mountains and the continental slope may force fluids originating on land to flow seawards. For example, a deep drilling transects in the shelf and slope environment of the southern Australian continental margin (Feary *et al.* 2000) suggested that fluids sampled in the platform and slope originated on the continent and migrated along stratigraphic boundary down slope. Such a scenario may explain seepage of fluid and hence heat flow anomalies at locations where aquifers outcrop on the slope. However, offshore Central Chile, the observed heat flow data do not support such a scenario. Thus, seawards of the

Table 1. Geothermal data (Grad: geothermal gradient, k: thermal conductivity, HF: heat flow).

Station	Longitude	Latitude	Depth [m]	Grad [K km^{-1}]	k[Wm^{-1} K^{-1}]	HF[m Wm^{-2}]
H0301	−72° 21.383′	−33° 28.317′	2012	32	1.06	34
H0301	−72° 20.246′	−33° 28.688′	1932	35	1.07	38
H0301	−72° 19.091′	−33° 28.884′	1859	43	1.07	46
H0301	−72° 18.087′	−33° 29.015′	1818	47	1.07	50
H0301	−72° 16.857′	−33° 29.331′	1667	53	1.07	57
H0301	−72° 15.709′	−33° 29.563′	1576	51	1.04	53
H0301	−72° 14.632′	−33° 29.802′	1494	50	1.05	52
H0301	−72° 13.512′	−33° 30.107′	1424	53	1.04	55
H0301	−72° 12.387′	−33° 30.343′	1349	58	1.02	59
H0301	−72° 11.238′	−33° 30.602′	1249	63	1.07	68
H0301	−72° 10.139′	−33° 30.867′	1165	79	1.07	85
H0301	−72° 9.005′	−33° 31.118′	1092	89	1.07	95
H0301	−72° 7.885′	−33° 31.371′	1007	104	1.09	114
H0302	−72° 24.906′	−33° 27.579′	2334	32	1.07	34
H0302	−72° 23.701′	−33° 27.803′	2215	32	1.07	34
H0302	−72° 22.541′	−33° 28.041′	2110	35	1.07	37
H0303	−72° 15.827′	−33° 30.102′	1557	48	1.07	51
H0303	−72° 15.910′	−33° 30.644′	1503	52	1.07	56
H0303	−72° 16.058′	−33° 31.059′	1526	52	1.07	55
H0303	−72° 16.215′	−33° 31.547′	1531	51	1.07	54
H0303	−72° 16.380′	−33° 32.043′	1554	52	1.07	56
H0303	−72° 16.531′	−33° 32.509′	1534	54	1.07	58
H0303	−72° 16.672′	−33° 32.993′	1532	52	1.07	56
H0303	−72° 16.825′	−33 °33.489′	1518	54	1.07	57
H0304	−73° 17.125′	−35° 16.078′	2026	45	0.88	40
H0304	−73° 16.080′	−35° 16.281′	2026	57	0.87	50
H0304	−73° 14.945′	−35° 16.605′	2083	62	0.91	57
H0304	−73° 13.735′	−35° 16.860′	2086	60	0.88	53
H0304	−73° 12.592′	−35° 17.225′	2096	62	0.84	52
H0304	−73° 11.487′	−35° 17.565′	2029	52	0.84	44
H0304	−73° 10.328′	−35° 17.911′	2044	61	0.88	54
H0304	−73° 9.208′	−35° 18.238′	1943	65	0.85	55
H0304	−73° 7.948′	−35° 18.624′	1958	77	0.85	66
H0304	−73° 6.888′	−35° 18.958′	1753	84	0.99	84
H0304	−73° 5.671′	−35° 19.254′	1311	71	1.02	73
H0304	−73° 4.538′	−35° 19.540	1140	81	1.03	83
H0304	−73° 3.380′	−35° 19.900′	970	100	1.03	102
H0304	−73° 2.258′	−35° 20.213′	808	138	1.03	142
H0307	−73° 31.637′	−35° 54.248′	1357	86	1.41	120
H0307	−73° 32.367′	−35° 54.231′	1435	95	1.42	135
H0307	−73° 33.158′	−35° 54.269′	1496	75	1.41	106
H0307	−73° 33.672′	−35° 54.266′	1480	NaN	NaN	NaN
H0307	−73° 34.431′	−35° 54.174′	1399	NaN	NaN	NaN
H0307	−73° 41.205′	−35° 54.486′	2214	NaN	NaN	NaN
H0307	−73° 40.305′	−35° 54.280′	2000	50	1.38	69
H0307	−73° 39.720′	−35° 54.259′	1852	50	1.38	69

location of fluid outflow, heat flow pattern should mimic the background flux. In contrast, the discrepancy between the background flux defined by the BSR-derived heat flow and the heat flow obtained at the seafloor increases landwards, which may indicate that the additional heat source is deep at the western terminus of the continental basement and approaches shallower depth towards the continent. We, therefore, suggest that fluids originate somewhere at depth and migrate laterally through the slope sediments upwards.

In recent models of earthquake nucleation and rupture propagation fluids are believed to play a major role (Sibson 1992; Byerlee 1993). Thus, elevated pore pressure lowers the effective stress on a fault and, therefore, may nurture earthquake rupture. After earthquake rupture, fluids will be redistributed, leading to post-seismic fluid flow. Post-seismic fluid flow has been inferred from the occurrence of aftershocks (Nur & Booker 1972) and time-dependent changes in the *P*-wave to *S*-wave velocity (v_p/v_s) ratios after the large 1995 Antofagasta subduction zone earthquake (Husen & Kissling 2001). Direct evidence for post-seismic fluid flow was reported from the great 1945 Makran subduction zone earthquake, where the thrust event caused intense mud volcano activity resulting in the creation of four new mud volcano islands, extensive venting of mud and gas along the coast and reactivation of onshore mud volcanoes (Sondhi 1947).

In central Chile, the region between 32°S and 37°S is known as an area with a strong potential for great ($M > 8$) underthrusting earthquakes (Kelleher 1972; Nishenko 1985). In the Valparaíso segment, between 32°S to ∼34°S, previous great earthquakes occurred in 1647, 1730, 1822 and 1906, and give an average repeat time of 86 +/−10 yr (Nishenko 1985). Furthermore, in 1971 and 1985 the city of Valparaíso was hit by large sized thrust faulting

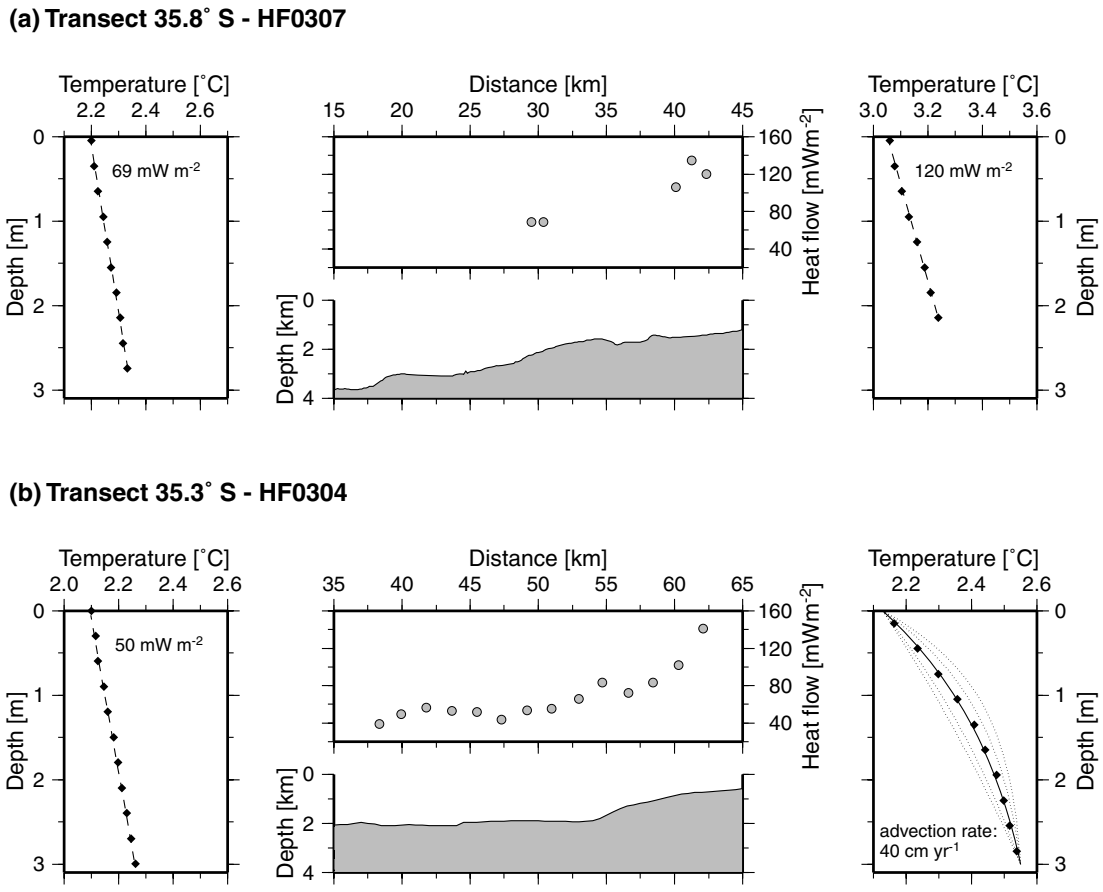

Figure 2. Heat flow data obtained along the two southern corridors. Data are displayed as function of distance from the trench axis. Measured temperature versus depth is shown for the most seaward and landward penetration. Temperature data show generally linear gradients, indicating conductive heat transfer. However, note the curved trend of the most landward penetration of station H0304, which can be explained by seepage at rates of $\sim$40 cm yr^{-1}.

earthquakes with magnitudes of $M = 7.5$ and $M = 7.8$, respectively (Christensen & Ruff 1986). The Talca segment between $\sim$34° and 37°S was hit by great earthquakes in 1570, 1657, 1751, 1835, 1928 and 1939 (Kelleher 1972). For the large 1995 Antofagasta event in northern Chile, Husen & Kissling (2001) provided evidence that the earthquake caused post-seismic fluid flow out of the subduction thrust into the forearc wedge. Constraints were derived from the inversion of traveltimes of aftershock data sets clearly separated in time, yielding a time evolution of high v_p/v_s ratios above the rupture plane. In their model, prior to earthquake rupture, high stress along the plate interface forms a permeability barrier, which keeps fluids trapped in the subduction thrust fault. After the earthquake, which breaks the barrier, a pressure gradient between lithostatic pore pressure along the plate interface and hydrostatic pore pressure in the overlying forearc crust induces fluid flow. Finite element modelling of such a scenario indicates that the release of lithostatic pressurized fluid trapped below the rupture plane (perhaps within the oceanic crust) can indeed explain the transient change is seismic velocity (Koerner *et al.* 2004). We, therefore, believe that fluids released by great and large subduction zone underthrust earthquakes may explain the observed heat flow pattern as a transient fluid flow phenomenon.

Fig. 3 shows the structure of the continental margin along the Valparaíso corridor at 33.5°S. Both multichannel seismic reflection data (Figs 3b and c) and seismic refraction data (Flueh *et al.* 1998; Zelt *et al.* 2003) indicate approximately 40 km landwards of the deformation front a major change in the structure of the forearc crust. Following previous interpretations (von Huene *et al.* 1997; Grevemeyer *et al.* 2003), we interpret this structural change as back stop. This change is most profound in seismic refraction data. Seismic velocity increases from $\sim$4 km s^{-1} in the accretionary prism to $>$5 km s^{-1} in the back stop. In Fig. 3(d) we have projected earthquakes (Engdahl & Villasenor 2002) that occur within a corridor of +/− 20 km along the seismic profile. To approximate the location of the seismogenic zone, we used the onset of seismicity as controlling parameter. Roughly 40–50 km from the deformation front, the number of earthquakes increases significantly. The onset of seismicity coincides with a temperature of 100°C isotherm at the plate boundary (Grevemeyer *et al.* 2003) and hence is expected to mark the updip limit of the seismogenic zone (Hyndman & Wang 1993). Therefore, evidence is accumulating that the updip limit of seismogenic behaviour offshore Valparaíso occurs roughly below the suture between the accretionary prism and the continental basement. Thus, if fluids trapped within the seismogenic zone are pushed into the overlying forearc crust following a large subduction earthquake (Husen & Kissling 2001; Koerner *et al.* 2004), the suture zone may promote focused flow from the plate boundary through the margin wedge.

The prominent heat flow anomaly in Central Chile occurs immediately landwards of the young accretionary wedge. Here, the BSR is disrupted (Fig. 4), which may indicate that warm fluids rising from depth pierce the BSR (Fig. 5). However, permeability in sedimentary

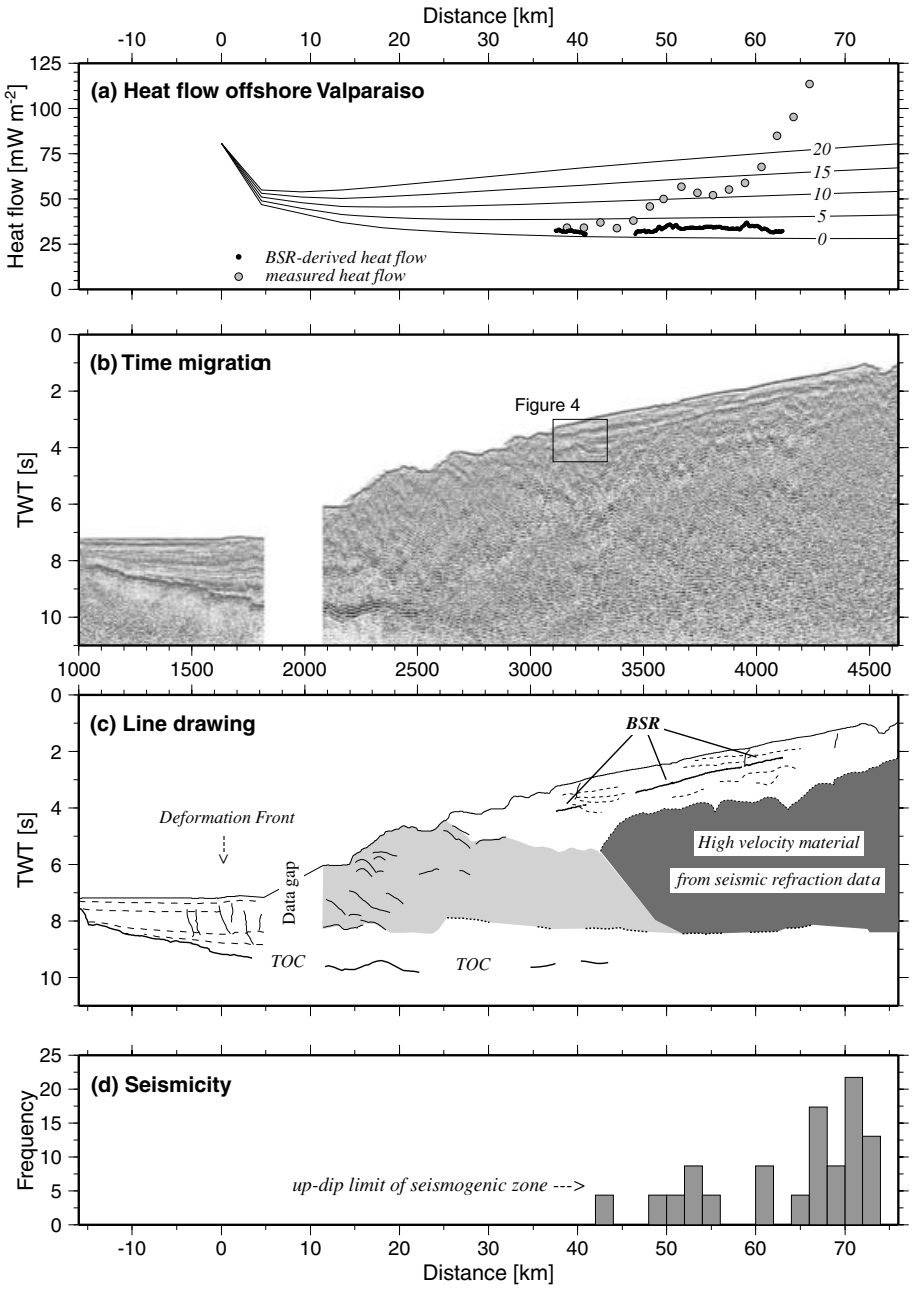

Figure 3. (a) Observed heat flow pattern along the Valparaíso corridor. BSR-derived data (black dots) show a flat trend across the slope and agree well with thermal subduction zone models (Grevemeyer *et al.* 2003). Measured heat flow values increase from values consistent with BSR-derived heat flow seawards and triple within 20–30 km landwards. Different amounts of shear heating in the subduction thrust (5 to 20 per cent of the lithostatic pressure) can not explain the observed trend. (b) Time-migrated seismic reflection data along the Valparaiso corridor and (c) Seismic line drawing and interpretation (Grevemeyer *et al.* 2003). High velocity body is derived from seismic refraction data (Flueh *et al.* 1998; Zelt *et al.* 2003). (d) Seismicity (Engdahl & Villasenor 2002) +/− 20 km projected on the seismic profile.

units is generally anisotrophic, with low permeability perpendicular to the strata and high values parallel to the bedding. Therefore, fluids may not rise directly vertically through the sedimentary apron, but flow laterally through the gas hydrate stability field until vertical pathways are provided. Landslides, normal faults, and other unconformities may generate such pathways. Thereby, volatiles may rise step by step through the gas hydrate field until they reach the seabed and seep out landwards of the suture zone. An area of seepage was perhaps sampled near the landward terminus of station H0304 near 35.3°S, where curved gradients indicate vertical fluid flow rates of 20–40 cm yr^{-1}. We expect that such large-scale episodic fluid flow events may inherently affect the distribution and concentration of natural gas hydrates in the slope sediments.

ACKNOWLEDGMENTS

We are grateful to Bernd Heesemann who did a great job during the sea-going programme and we appreciate the excellent support of Commander Davanzo and his crew of the Chilean Navy

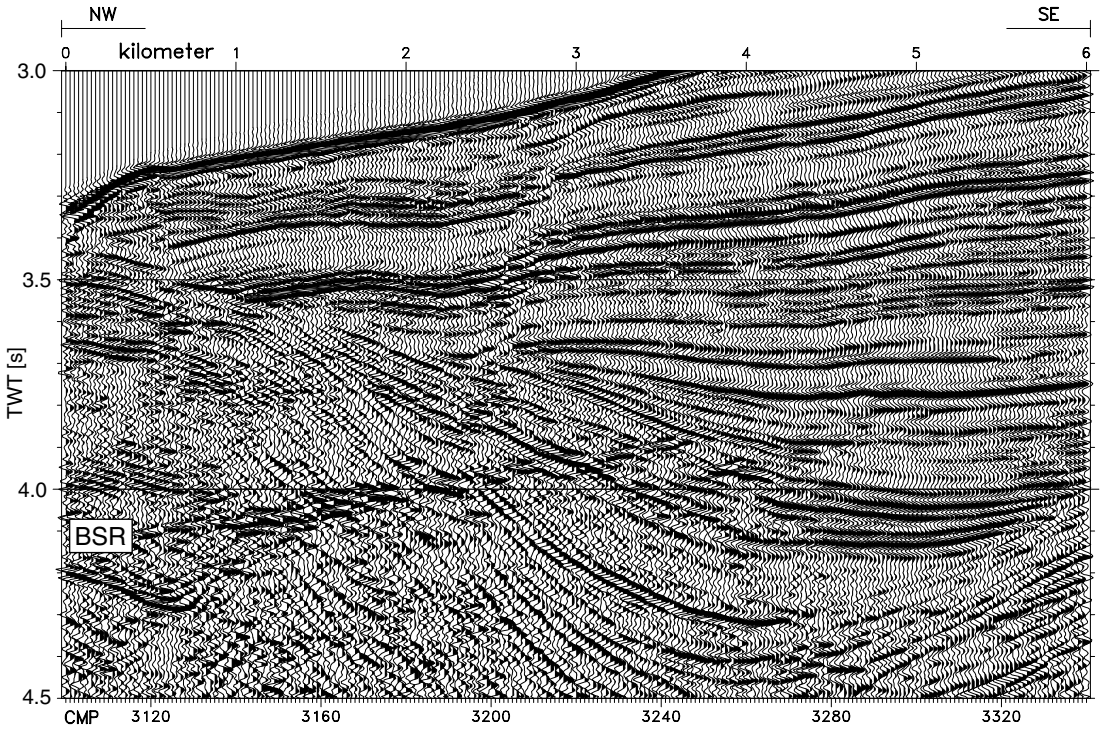

Figure 4. Detailed blow-up of the seismic section indicating the area where the bottom simulating reflector (BSR) disappears. See Fig. 3(b) for location.

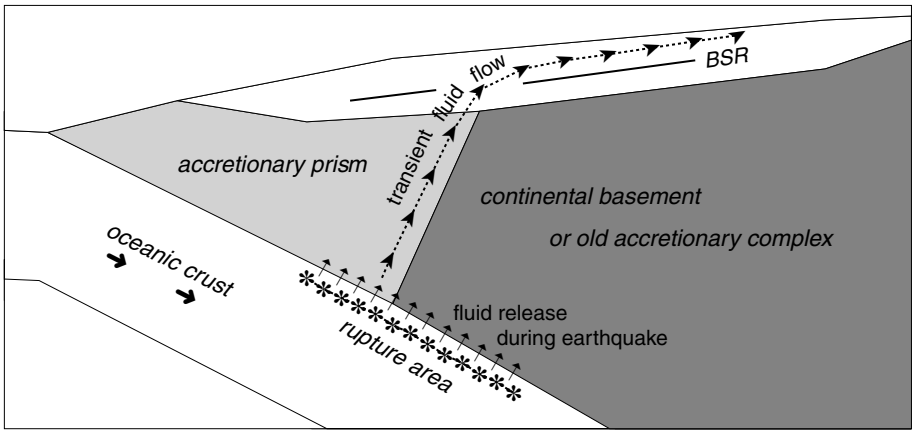

Figure 5. Model for transient fluid flow. Fluids captured in the subduction thrust are released during large and great earthquakes and migrate along structurally controlled boundaries through the margin wedge. See text for further discussion.

research vessel *Vidal Gormaz.* This study was supported by the Deutsche Forschungsgemeinschaft (DFG grant Gr 1964/3-1), a Chilean-German bilateral cooperation in Science and Technology (DLR-BMBF Grant CL00/006 to IG and DRI-CONICYT Grant 2000-138 to JD), and by FONDEF through the programme '*Hidratos de gas submarinos: una nueva fuente de energía para el siglo XXI'* (FONDEF Grant D00I11004). César Ranero provided the time migrated data from profile SO104p1 shown in Figs 3 and 4. Constructive reviews from Achim Kopf and Tim Minshull are greatly appreciated.

REFERENCES

Bangs, N.L. & Cande, S.C., 1997. Episodic development of a convergent margin inferred from structures and processes along the southern Chile margin, *Tectonics,* **16,** 489–503.

Bredehoeft, J.D. & Papadopulos, I.S., 1965. Rates of vertical ground water movement estimated from the earth's thermal profile, *Water Resources Res.,* **1,** 325–328.

Byerlee, J., 1993. Model for episodic flow of high -pressure water in fault zones before earthquakes. *Geology,* **21,** 303–306.

Christensen, D.H. & Ruff, L.J., 1986. Rupture process of the March 3, 1985 Chilean earthquake, *Geophys. Res. Lett.,* **13,** 721–724.

Davis, E.E., Hyndman, R.D. & Villinger, H., 1990. Rates of fluid expulsion across the northern Cascadia accretionary prism: constraints from new heat flow and multichannel seismic reflection data, *J. geophys. Res.,* **95,** 8869–8889.

DeMets, C., Gordon, R.G., Argus, D.F. & Stein, S., 1994. Effect of recent revisions to the geomagnetic reversal time-scale on estimates of current plate motions, *Geophys. Res. Lett.,* **21,** 2191–2194.

Engdahl, E.R. & Villasenor, A., 2002. Global seismicity: 1900–1999, *International Handbook of Earthquake and Engineering Seismology,* **81A,** 665–690.

Feary, D.A., Hine, A.C., Malone, M.J. *et al.*, 2000. *Proceeding of the Ocean Drilling Program, Initial Reports,* **182,** Site 1129, 1–86.

Foucher, J.P., LePichon, X., Lallemant, S., Hobart, M.A., Henry, P., Benedetti, M., Westbrook, G. & Langseth, M.G., 1990. Heat flow, tectonics, and fluid circulation at the toe of the Bartbados accretionary prism, *J. geophys. Res.,* **95,** 8859–8867.

Fisher, A.T. & Hounslow, M.W., 1990. Transient fluid flow through the toe of the Barbados accretionary complex: constraints from Ocean Drilling Program Leg 110 heat flow studies and simple models, *J. geophys. Res.,* **95,** 8845–8858.

Flueh, E.R., Vidal, N., Ranero, C.R., Hojka, A., von Huene, R., Bialas, J., Hinz, K., Cordoba, D., Danobeitia, J.J. & Zelt, C., 1998. Seismic investigations of the continental margin off- and onshore Valparaiso, *Tectonophysics,* **288,** 251–263.

Ganguly, N., Spence, G.D., Chapman, N.R. & Hyndman, R.D., 2000. Heat flow variations from bottom simulating reflectors on the Cascadia margin, *Mar. Geol.,* **164,** 53–68.

Grevemeyer I., Diaz-Naveas, J.L., Ranero, C.R., Villinger, H. & Ocean Drilling Program Leg 202 Scientific Party, 2003. Heat flow over the descending Nazca plate in Central Chile, 32°S to 41°S: evidence from ODP Leg 202 and the occurrence of natural gas hydrates, *Earth Planet. Sci. Lett.,* **213,** 285–298.

Grevemeyer, I. *et al.*, 2004. Fluid flow through active mud dome Mound Culebra offshore Costa Rica: evidence from heat flow surveying, *Mar Geol.,* **207,** 145–157.

Harrison, J.V., 1944. Mud volcanoes on the Makran coast, *Geogr. J.,* **103,** 180–181.

Hartmann, A. & Villinger, H., 2002. Inversion of marine heat flow measurements by expansion of the temperature decay function, *Geophys. J. Int.,* **148,** 628–636.

Hyndman, R.D. & Wang, K., 1993. Thermal constraints on the zone of major thrust earthquake failure: the Cascadia subduction zone, *J. geophys. Res.,* **98,** 2039–2060.

Husen, S. & Kissling, E., 2001. Postseismic fluid flow after the large subduction zone earthquake of Antofagasta, Chile, *Geology,* **29,** 847–850.

Kelleher, J.A., 1972. Rupture of large south American earthquakes and some predictions, *J. geophys. Res.,* **77,** 2087–2103.

Koerner, A., Kissling, E. & Miller, A., 2004. A model of deep crustal fluid flow following the $Mw = 8.0$ Antofagasta, Chile, earthquake, *J. geophys. Res.,* **109,** doi:10.1029/2003JB002816.

Kopf, A.J., 2002. Significance of mud volcanism. *Rev. Geophysics,* **40**(2), 1005, doi:10.1029/2000RG000093.

Kopf, A., Klaeschen, D. & Mascle, J., 2001. Extreme efficiency of mud volcanism in dewatering accretionary prisms, *Earth Planet. Sci. Lett.,* **189,** 295–313.

Molnar, P. & England, P., 1990. Temperature, heat flux, and frictional stress near major thrust faults, *J. geophys. Res.,* **95,** 4833–4856.

Moore, J.C. & Vrolijk, P., 1992. Fluids in accretionary prisms. *Rev. of Geophysics,* **30**(2), 113–135.

Mordojovich, C., 1974. Geology of a part of the Pacific margin of Chile. in eds Burk, C.A. & Drake, C.L., *The Geology of Continental Margins*, pp. 591–598, Springer Verlag, New York.

Nishenko, S.P., 1985. Seismic potential for large and great earthquakes along the Chilean and southern Peruvian margins of south America: a quantitative reappraisal, *J. geophys. Res.,* **90,** 3589–3616.

Nur, A. & Booker, J.R., 1972. Aftershocks caused by pore fluid flow? *Science,* **175,** 885–887.

Oleskevich, D.A., Hyndman, R.D. & Wang, K., 1999. The updip and downdip limits to great subduction earthquakes: thermal and structural models of Cascadia, south Alaska, SW Japan, and Chile, *J. geophys. Res.,* **104,** 14 965–14 991.

Pankhurst, R.J., Hervé, M., Rojas, L. & Cembrano, J., 1992. Magmatism and tectonics in continental Chiloe, Chile (42°–42°30′S), *Tectonophysics,* **205,** 283–294.

Ruff, L.J., 1996. Large earthquakes in subduction zones: segment interaction and recurrence times. in eds Bebout, G.E., Scholl, D.W., Kirby, S.H. & Platt, J.P., Subduction – Top to Bottom, *Geophysical Monograph*, **96**, 91–104.

Sibson, R.H., 1992. Implications for fault-value behaviour for rupture nucleation and recurrence, *Tectonophysics,* **211,** 283–293.

Sondhi, V.P., 1947. The Makran earthquake, 28th November 1945: the birth of new islands, *Indian Miner.,* **1**(3), 147–154.

Villinger, H., Grevemeyer, I., Kaul, N., Hauschild, J. & Pfender, M., 2002. Hydrothermal heat flux through aged oceanic crust: where does the heat escape? *Earth Planet. Sci. Lett.,* **202,** 159–170.

von Huene *et al.*, 1997. Tectonic control of the subducting Juan Fernández Ridge on the Andean margin near Valparaiso, Chile, *Tectonics,* **16**, 474–488.

Wood, W.T., Gettrust, G.E., Chapman, N.R., Spence, G.D. & Hyndman, R.D., 2002. Decreased stability of methane hydrates in marine sediments owing to phase-boundary roughness, *Nature,* **420,** 656–660.

Zelt, C.A., Sain, K., Naumenko, J.V. & Sawyer, D.S., 2003. Assessment of crustal velocity models using seismic refraction and reflection tomography, *Geophys. J. Int.,* **153,** 609–626.